processes

MDPI

Article

Experimental Study on Microwave Pyrolysis of Decommissioned Wind Turbine Blades Based on Silicon Carbide Absorbents

Dongwang Zhang [1,2], Qiang Song [2], Bo Hou [3], Man Zhang [2], Da Teng [3], Yaning Zhang [1], Rushan Bie [1,*] and Hairui Yang [2,*]

[1] School of Energy Science and Engineering, Harbin Institute of Technology, Harbin 150001, China; 18810551680@163.com (D.Z.); ynzhang@hit.edu.cn (Y.Z.)
[2] Key Laboratory of Thermal Science and Power Engineering of Ministry of Education, Department of Energy and Power Engineering, Tsinghua University, Beijing 100084, China; qsong@mail.tsinghua.edu.cn (Q.S.); zhangman@mail.tsinghua.edu.cn (M.Z.)
[3] China Energy Longyuan Environmental Protection Co., Ltd., Beijing 100039, China; 12068059@ceic.com (B.H.); tengda8013@163.com (D.T.)
* Correspondence: rushan@hit.edu.cn (R.B.); yhr@mail.tsinghua.edu.cn (H.Y.); Tel.: +86-13946013563 (R.B.); +86-13691058057 (H.Y.)

Abstract: The rapid expansion of the scale of wind power has led to a wave of efforts to decommission wind turbine blades. The pyrolysis of decommissioned wind turbine blades (DWTBs) is a promising technological solution. Microwave pyrolysis offers the benefits of fast heating rates and uniform heat transfer, making it a widely used method in various heating applications. However, there are few studies on the microwave pyrolysis of DWTBs, and pyrolysis characteristics under different boundary conditions remain unclear. In this paper, we investigate the pyrolysis characteristics of DWTBs by utilizing silicon carbide (SiC) particles as a microwave absorbent. The results demonstrated that, when the microwave heating power increased from 400 W to 600 W, the heating rate and pyrolysis final temperature of the material increased, resulting in a reduction in pyrolysis residual solid yield from 88.30% to 84.40%. At 600 W, pyrolysis gas components included C_2H_4, CH_4, and CO, while the tar components included phenol and toluene. The highest degree of pyrolysis was achieved under the condition of an SiC particle size of 0.85 mm, with better heating performance, and the calorific value of the pyrolysis gas generated was 36.95 MJ/Nm^3. The DWTBs did not undergo pyrolysis when SiC was not added. However, when the mass ratio of SiC to DWTBs was 4, the tar yield was 4.7% and the pyrolysis gas yield was 17.0%, resulting in a faster heating rate and the highest degree of pyrolysis. Based on this, an optimal process for the microwave pyrolysis of DWTBs was proposed, providing a reference for its industrial application.

Keywords: microwave pyrolysis; decommissioned wind turbine blades; heating power; particle size; SiC loading

Citation: Zhang, D.; Song, Q.; Hou, B.; Zhang, M.; Teng, D.; Zhang, Y.; Bie, R.; Yang, H. Experimental Study on Microwave Pyrolysis of Decommissioned Wind Turbine Blades Based on Silicon Carbide Absorbents. *Processes* **2024**, *12*, 1065. https://doi.org/10.3390/pr12061065

Academic Editors: Ming-Hsun Cheng, Kurt A. Rosentrater, Amin Mirkouei and Ramkrishna Singh

Received: 24 April 2024
Revised: 17 May 2024
Accepted: 21 May 2024
Published: 23 May 2024

1. Introduction

In order to respond actively to climate change and promote green and low-carbon development, the world energy system is transitioning towards a near zero emission model, with a particular focus on advancing the renewable energy sector. Among various green, clean, and sustainable energy sources, wind energy has emerged as a particularly promising option due to its advantages of widespread availability, a quick installation process, low operation and maintenance costs, and high efficiency in power generation. The global installed capacity of wind turbines has increased exponentially, from 17 GW in 2000 to 923 GW in 2020 [1,2]. This represents a more than 50-fold increase, and the annual installed capacity continues to maintain a high growth trend. Wind power will continue to play

a leading role in the new energy system and will also play an important role in future energy systems.

Wind turbine blades play a pivotal role in the conversion of wind energy into mechanical power. They are also the most costly component in the wind turbine, with a designed service life of 20 to 25 years [3]. With the rapid expansion of the total installed capacity of wind power and the implementation of technical transformation programs such as "replacing small with large units", the old wind turbine blades are undergoing a climax of retirement worldwide [4]. It is predicted that the retired wind turbine blade volume will reach a peak of 500,000 tons per year in 2029. With the rapid growth of the installed capacity of wind turbines, the weight of global wind turbine blades will reach 43.4 million tons in 2050 [5]. The decommissioning of blades presents a significant challenge in terms of their disposal. Conventional methods, such as landfilling and incineration, have the potential to cause environmental harm and contribute to the depletion of resources. Consequently, there is an urgent need to develop more efficient and eco-friendly blade disposal techniques in order to achieve the sustainable and circular development of the wind power industry.

Glass-fiber-reinforced composite (GFRC) is currently the most prevalent material used in wind turbine blades due to its characteristics of high strength, high stiffness, and low cost characteristics. It accounts for more than 90% of the total blade mass [6,7]. GFRC can be regarded as a composite material of resin and glass fiber, where the resin acts as matrix to balance the load and protect the glass fiber, and the glass fiber acts as a reinforcing material to improve overall mechanical properties. The resin is chemically cross-linked with the glass fiber during the curing process, and the complexity of the curing process and the irreversibility of the cross-linking process make it difficult to degrade and recycle the blades by remelting or reshaping them after decommissioning.

At present, blade recovery technologies are mainly divided into three categories: mechanical recovery, chemical solvent recovery, and pyrolysis recovery [8–13]. The mechanical method cannot achieve a reduction in blade solid waste and cannot recover fiber for reuse; chemical solvent recovery requires high-temperature and high-pressure conditions, consuming a large amount of energy; and the waste liquid after recovery is difficult to handle. Compared with the mechanical method and the chemical solvent method, the pyrolysis method can realize the cracking and separation of the resin at medium- and low-temperature conditions, recover the glass fiber more completely, generate combustible gas and liquid tar in the process, and better preserve the mechanical properties of the fiber. Thus, they can meet the requirements of the circular economy and become one of the most promising technologies for the treatment of decommissioned wind turbine blades [14–18].

In the pyrolysis method, microwave pyrolysis can realize the heating of the material from inside to outside, and the resin of the blade can quickly absorb the microwave radiation energy, thus increasing the decomposition rate. The energy requirement for conventional pyrolysis of wind turbine blades is about 21.2 MJ/kg [19], while microwave pyrolysis requires only about 10 MJ/kg [20]. Therefore, microwave pyrolysis has attracted considerable attention from scholars in recent years due to its advantages of a fast heating rate and a low processing energy consumption. Deng et al. [21] investigated the recovery of fiber in composites via microwave pyrolysis, and the fiber obtained had a smoother surface and shorter reaction time and the chemical structure of the fiber was not significantly changed. Åkesson et al. [22] pyrolyzed glass-fiber-reinforced composites via microwaving, yielding pyrolytic oil with a high caloric value of 36 MJ/kg. Dan et al. [23] carried out microwave pyrolysis of shredded wind turbine blades. The recovered fiber lost only 25% of its strength, which enabled its use producing non-woven fiber felt. Hao et al. [24] observed coke residue on the surface of the fiber that was recovered via pyrolysis, and obtained relatively clean and complete fibers after oxidation treatment. The oxygen-containing groups in the recovered fibers increased. Ren et al. [25] proposed a microwave pyrolysis oxidation process for the rapid recovery of carbon fiber, and the obtained regenerated carbon fiber had a tensile strength retention rate of 99.42% and a tensile modulus retention rate of 96.5%. At the same time, the fiber recovered via microwave pyrolysis had poor

adhesion to the base material, which could be improved by maleic anhydride-grafted polypropylene [26]. However, due to the poor wave-absorbing ability of resin and other materials, microwave absorbent can be added to improve the heating effect. Studies have shown that SiC has a wide wave absorption band and chemical stability in high-temperature environments. As such it is recognized as an effective absorbent [27–29] that can achieve the rapid heating of materials. However, there are no relevant reports on the use of SiC as an absorbent in the pyrolysis of wind turbine blades. In order to reduce energy consumption via pyrolysis, the microwave pyrolysis characteristics of decommissioned wind turbine blades, using SiC as an absorbent, were investigated in this paper. Additionally, the effects of the key parameters affecting microwave heating, including microwave heating power, SiC particle size, and SiC loading, for the pyrolysis of wind turbine blades were analyzed. This provides important technical and data support for the subsequent large-scale and resourceful application of microwave pyrolysis for decommissioned wind turbine blades.

2. Materials and Methods

2.1. Materials

Figure 1 depicts the decommissioned wind turbine blade (DWTBs) and SiC particles utilized in the experiment. The DWTBs were sourced from a commercial wind farm in China and served as the primary ingredient, namely, glass fiber-reinforced composite (GFRC). Then, they were subsequently cut into 10 × 10 × 10 mm blocks. The SiC was supplied by Hebei Qinghe Andy Metal Material Co., Ltd (Xingtai. China). The DWTBs employed in the experiment were primarily composed of E-glass fibers (76.5 wt%) and bisphenol A-type epoxy cured by amines (23.5 wt%), exhibiting a density of 1.99×10^3 kg/m^3. Table 1 presents the proximate analysis and ultimate analysis of DWTBs, which was performed using an industrial analyzer (Thermostep, Krohne, Germany) and an elemental analyzer (Vario EL III, Hanau, Germany), revealing a notably high ash content of 76.4%. The ash predominantly comprises glass fiber with a high melting point and is difficult to degrade naturally, consequently resulting in its low calorific value. Table 2 illustrates the XRF analysis of DWTBs, obtained by a X-ray fluorescence spectrometer (SPECTRO XEPOS, Kleve, Germany), in which the main elements are Si, Ca, Al, etc. The density and purity of SiC as a microwave absorbent were 3.23×10^3 kg/m^3 and 97%, respectively. The absorbent was sieved into five particle levels with a standard sieve according to the experimental demand, with the median particle sizes being 0.06 mm, 0.09 mm, 0.85 mm, 2 mm, and 3 mm, respectively.

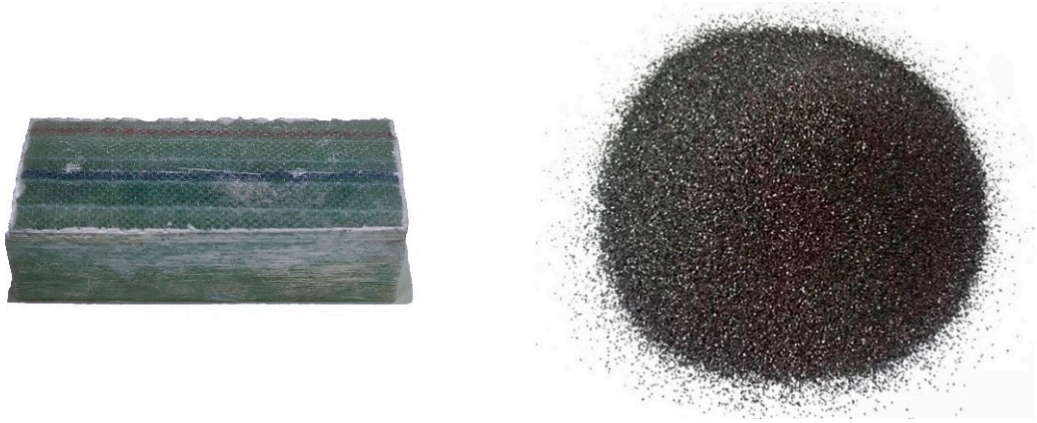

(**a**) (**b**)

Figure 1. Picture of wind turbine blade and SiC. (**a**) Wind turbine blade; (**b**) SiC particle.

Table 1. Proximate analysis and ultimate analysis of DWTBs.

Proximate Analysis/Mass%				Ultimate Analysis/Mass%					Low Calorific Value
M_{ar}	A_{ar}	V_{ar}	FC_{ar}	C_{ar}	H_{ar}	O_{ar}	N_{ar}	S_{ar}	$Q_{net.ar}$/kJ/kg
0.23	76.4	22.25	1.12	15.89	2.19	4.79	0.714	0.02	7119.7

Table 2. XRF analysis of DWTBs material.

Compound	SiO_2	CaO	Al_2O_3	MgO	TiO_2	Cl	Fe_2O_3	K_2O
Mass ratio/%	56.282	15.508	14.618	8.775	1.907	1.042	0.697	0.592

2.2. Experimental System

Figure 2 illustrates the microwave pyrolysis experimental system, comprising a microwave heating device, vacuum pumping device, temperature monitoring device, reaction kettle, condensation tube, and gas bag. The microwave heating device, manufactured by Longyu Co., Ltd. (Nanyang, China), had a maximum power of 1000 W, an accuracy of 1 W, and a microwave frequency of 2450 MHz. The temperature monitoring device was employed to monitor the temperature change of the material in the reactor in real time. The reactor was constructed from quartz glass and had a capacity of 100 mL. The pyrolysis product was passed from the reactor to the condenser device via the connecting tube, and the tar was cooled down sufficiently using iced water and condensed for GC-MS (QC-MS) analysis. The pyrolysis gas, collected in the bag, was analyzed by gas mass spectrometry (LC-D200M Tilon, UT, USA) and a portable infrared gas analyzer (Gasboard-3100P, Wuhan, China).

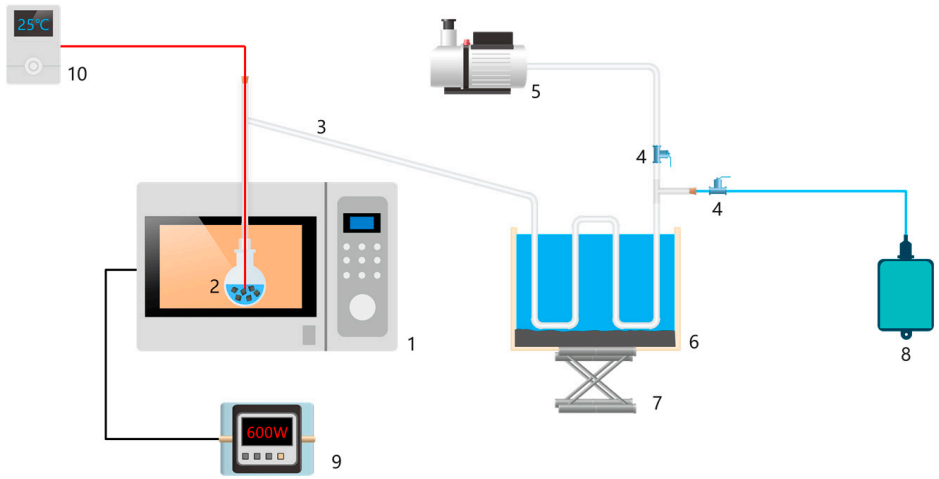

Figure 2. Schematic diagram of microwave pyrolysis experimental equipment: (1) microwave heating device, (2) reaction kettle, equipped with DWTBs and SiC, (3) connecting tube, (4) valve, (5) vacuum pump, (6) tar condensing device, (7) bracket, (8) gas bag, (9) power monitor (the accuracy is 0.001 w), and (10) temperature monitoring device (the accuracy is 0.001 °C).

2.3. Experimental Procedures

The objective of this study was to investigate the impact of microwave power, microwave absorbent particle size, and microwave absorbent loading on the gas and oil production characteristics of DWTBs pyrolysis. Table 3 outlines the experimental conditions tested in this study. It was demonstrated in previous studies that glass fiber exhibited thermal stability within a temperature range of 30–900 °C [30], whereas resin was unable to undergo pyrolysis reactions at a temperature below 400 °C [31]. At temperatures above 500 °C, the pyrolysis process was significantly accelerated, resulting in the production of a considerable quantity of aromatic chemicals [32]. The results of microwave pyrolysis

research indicated that a microwave heating power from 400 to 600 W was necessary to ensure adequate pyrolysis of resin and prevent excessive damage to the strength of the glass fiber. Jing et al. [33] demonstrated that the amount of absorbent had an impact on the temperature distribution of the system, while Fan et al. [34] showed that an appropriate amount of absorbent could promote the pyrolysis process. In this study, the loading capacity of SiC was set in the range of 0–80 g. Liu et al. [35] demonstrated that the energy absorption efficiency of materials was influenced by the particle size of the absorbent. In this study, five SiC particle sizes were selected in order to investigate their impact on pyrolysis characteristics.

Table 3. Experimental design of SiC-assisted microwave pyrolysis of DWTBs.

Run	Microwave Power (W)	Sic Loading Capacity (g)	Sic Particle Size (mm)
Run 1	400	80	0.85
Run 2	450	80	0.85
Run 3	500	80	0.85
Run 4	550	80	0.85
Run 5	600	80	0.85
Run 6	600	80	2
Run 7	600	80	3
Run 8	600	80	0.09
Run 9	600	80	0.06
Run 10	600	60	0.85
Run 11	600	40	0.85
Run 12	600	20	0.85
Run 13	600	0	0.85

Prior to the commencement of the experiment, 20 g of DWTBs was added to the reactor, the mass of DWTBs was recorded as W_0, and then SiC was added and mixed evenly. The mass of the reactor after loading DWTBs and SiC was recorded as W_{10}, and the mass of the thermocouple, condensing tube, and connecting tube before the reaction was W_{20}. The reactor, thermocouples, condenser tubes, vacuum pump, and gas bag were connected in accordance with the configuration depicted in Figure 2. The reaction kettle in the microwave heating device was insulated with quartz cotton, and ice was added to the condensing device to ensure a cooling effect. Initially, the vacuum pump was activated to remove air from the reaction vessel and pipeline, thereby creating an oxygen-free atmosphere. Subsequently, the microwave heating device, temperature monitoring device, and power monitor were activated, and the heating device was deactivated when no pyrolysis gas was produced. Finally, the mass of the reaction vessel with DWTBs and SiC after the reaction was weighed as W_{11}, and the mass of the thermocouple, condensing tube, and connecting tube after the reaction was W_{21}. The pyrolysis gas, tar, and solid yields were calculated according to the following formula:

$$Y_{\text{oil}} = \frac{W_{21} - W_{20}}{W_0} \times 100\% \quad (1)$$

$$Y_{\text{gas}} = \frac{(W_{10} - W_{11}) - (W_{21} - W_{20})}{W_0} \times 100\% \quad (2)$$

$$Y_{\text{solid}} = 1 - Y_{\text{oil}} - Y_{\text{gas}} \quad (3)$$

where Y_{oil}, Y_{gas}, and Y_{solid} are tar, pyrolysis gas, and pyrolysis solid yields (%), respectively.

3. Results and Discussion

3.1. Effect of Microwave Heating Power on Pyrolysis Products

3.1.1. Gas Yield and Oil Yield at Different Microwave Heating Power

Figure 3 illustrates the gas, oil, and solid yield under different microwave heating powers (in Run 1~Run 5, the SiC loading is 80 g and the particle size is 0.85 mm). The combined yield of tar and pyrolysis gas increased from 15.60% to 21.70% as the microwave heating power increased from 400 W to 600 W. Pyrolysis gas and tar exhibited high calorific values, and the increase in their combined yields also indicated that the increase in microwave heating power increased the pyrolysis degree. At a lower microwave heating power, insufficient energy was available to break the molecular bonds of the resin, resulting in a higher solid yield, which aligned with the research law of Fan et al. [36].

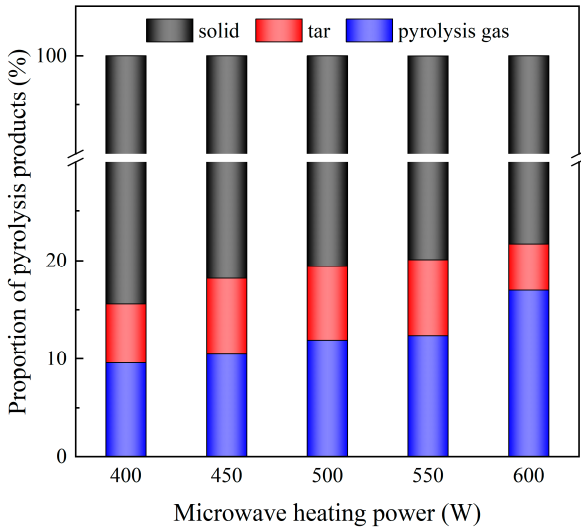

Figure 3. Mass ratio of pyrolysis products under different microwave heating power (the SiC loading is 80 g, and the particle size is 0.85 mm).

The increase in microwave heating power resulted in a monotonic increase in pyrolysis gas yield, while the tar yield displayed an initial increase, followed by a decrease. At higher levels of microwave heating power, the peak heating temperature and pyrolysis termination temperature increased due to the uneven temperature distribution and heat delay inside the DWTBs [37,38], which was conducive to the promotion of the pyrolysis process and a reduction in the pyrolysis coke yield. Concurrently, elevated microwave heating power expedited the heating rate and reduced the duration of pyrolysis, thereby facilitating the formation of volatile products. However, when the microwave heating power continued to increase, the secondary pyrolysis of tar and other macromolecular substances led to a decline in the tar yield [39], while the pyrolysis gas yield increased rapidly, which was in accordance with the observations of Fagbemi et al. [40,41].

3.1.2. Gas Component at Different Microwave Heating Power

Figure 4 illustrates the variations in pyrolysis gas components under different microwave heating powers. It was evident that the primary components of pyrolysis gas included C_2H_4, CH_4, O_2, CO_2, C_3H_8, H_2, etc. The percentage of C_2H_4 in pyrolysis gas was the highest, reaching 44.1%. When the microwave heating power reached 550 W, the output of C_2H_4 began to decrease, indicating that the re-pyrolysis effect began to be obvious at this time, thus generating CH4 and CO. It is noteworthy that the pyrolysis gas exhibited a higher concentration of O_2, with a range from 13.08% to 17.09%. This phenomenon may be attributed to the breaking of chemical bonds in resin molecules, such as C-H, C-C, and C-O, at elevated temperatures. This process results in the formation of numerous oxygen-containing free radicals, which subsequently react to generate O_2.

Furthermore, the breaking of oxygen-containing chemical bonds released oxygen atoms or small molecules containing oxygen (such as CO, CO_2), which recombined to form O_2 through a series of intermediate reactions. The vacuum conditions facilitated gas escape and cooling, reducing the possibility of oxygen reacting with other substances while enhancing oxygen generation. At the same time, the equipment limitations precluded the complete realization of the vacuum environment, resulting in a residual oxygen content that contributed to a slight increase in oxygen production. In practical industrial pyrolysis equipment, it is recommended to extend the residence time of pyrolysis gas for as long as possible to prevent the risk of explosion.

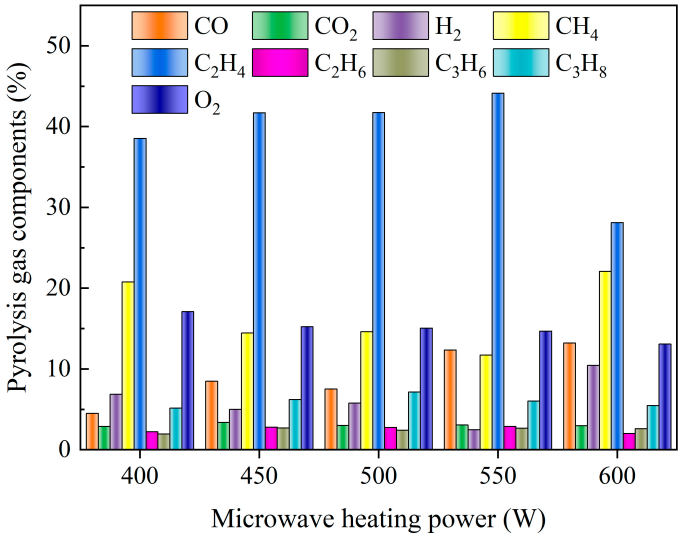

Figure 4. Pyrolysis gas components under different microwave heating power (the SiC loading is 80 g, and the particle size is 0.85 mm).

Figure 5 presents the calorific value (Q_{net}—determined based on the weighted calorific value of the single gas and the composition of pyrolysis gas) and the converted heat ($Q_{net,total}$—the energy converted according to the mass of pyrolysis gas components) of pyrolysis gas under different microwave heating powers, which are calculated according to equations 4 and 5. It can be observed that the calorific value of the gas exhibited an initial increase and subsequent decline with the rise in microwave heating power. This phenomenon could be attributed to the fact that with the enhancement of microwave heating power, the degree of resin pyrolysis initially increased, resulting in the enhanced production of C_2H_4 with a high calorific value. Subsequently, as the microwave heating power continued to increase, the re-pyrolysis effect of the tar became more pronounced. It was inferred that low molecular weight substances, such as H_2 and CH_4, were produced by the tar re-pyrolysis.

$$Q_{net} = \sum Q^i{}_{net} \times f^i \quad (4)$$

$$Q_{net,total} = \sum Q^i{}_{net} \times V^i \quad (5)$$

where $Q^i{}_{net}$ is the unit calorific value of each component gas (J/Nm^3), and f^i and V^i are the volume proportion (%) and volume amount (Nm^3) of each component gas.

3.1.3. Temperature Rise Characteristic at Different Microwave Heating Power

Figure 6 illustrates the temperature rise curve of the material under different microwave heating powers. It was evident that an increase in microwave heating power resulted in an accelerated heating rate and a higher final temperature (the temperature at 25 min) of SiC and DWTBs. With an increase in power from 400 W to 600 W, the temperature of the system increased from 450 °C to 670 °C. The accelerated heating rate proved to

be advantageous in terms of enhancing the maximum weight loss rate and reducing the reaction time. When a higher heating power was used, due to the shorter pyrolysis time required, the pyrolysis heat absorption became less obvious in the later stage, and so there was a small temperature rise process at about 20 min.

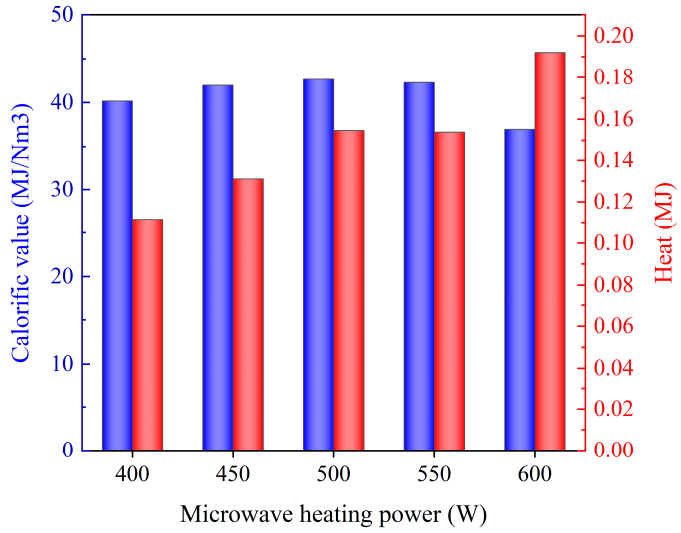

Figure 5. Calorific value and heat of pyrolysis gas under different microwave heating powers: the SiC loading is 80 g, and the particle size is 0.85 mm.

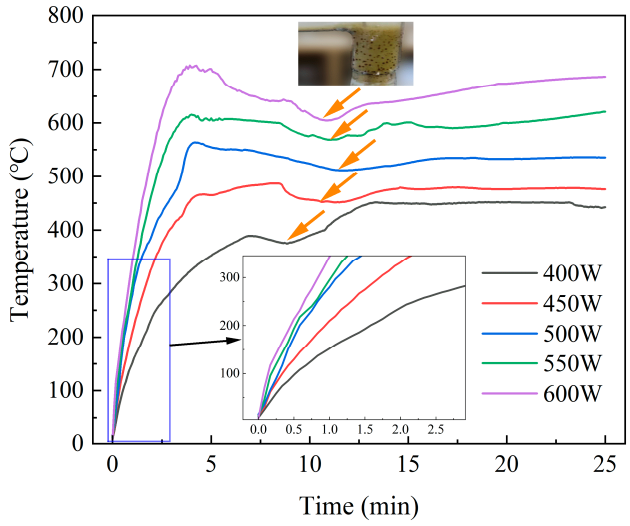

Figure 6. Temperature rise curves of the material under different microwave heating power (the SiC loading is 80 g, and the particle size is 0.85 mm).

In actual industrial applications, it is not advisable to pursue high microwave heating power without consideration of the relevant factors. A high microwave heating power can lead to a high pyrolysis temperature, which in turn can accelerate the generation and expansion of fiber defects. This results in a sharp decline in the tensile strength of fiber after pyrolysis [42,43], limiting its secondary use. Furthermore, the prolongation of pyrolysis time can promote the pyrolysis of resin, but will also reduce the mechanical properties of fiber [44]. In this study, the experiment was terminated when the pyrolysis gas flow fell below a specified threshold of 10 mL/min.

Additionally, it was observed in the experiment that there was a minor temperature drop during the pyrolysis process, as indicated by the orange arrow in Figure 6. Studies by Wu et al. [45] revealed that the pyrolysis of resin reached its maximum value at 400 °C. In this study, since resin pyrolysis is an endothermic reaction, the temperature drop stage

corresponds to the most intense stage of the pyrolysis process. At this stage, the color of the volatile products can be observed to be darker, as shown in the dark yellow part at the top of Figure 5, which further verifies that there is a high pyrolysis rate at this stage.

3.2. Effect of Particle Size of Absorbent (SiC) on Pyrolysis Products

3.2.1. Gas Yield and Oil Yield at Different SiC Size

Figure 7 illustrates the mass distribution of pyrolysis products under different SiC particle sizes (Run 5~Run 9, the SiC loading is 80 g, and microwave power is 600 W). It can be observed that as, the size of SiC particle increased, the total amount of tar and pyrolysis gas generated by pyrolysis initially increased and then decreased. It was found that there existed an optimal particle size that maximized the pyrolysis efficiency of DWTBs. The smaller the SiC particles, the more likely they were to be distributed in the bottom of the reactor, and the worse overall contact effect was, resulting in a weaker microwave absorption ability. Although the small particles enhanced heat exchange with DWTBs, the overall heat absorption capacity of the system still needed to be improved. The heating rate of SiC is 15.6–77.2 times higher than that of plastic material under the same conditions [46]. Conversely, a larger particle size provided an enhanced heat absorption capacity. However, the decreased specific surface area impaired heat transfer efficiency of SiC and DWTBs.

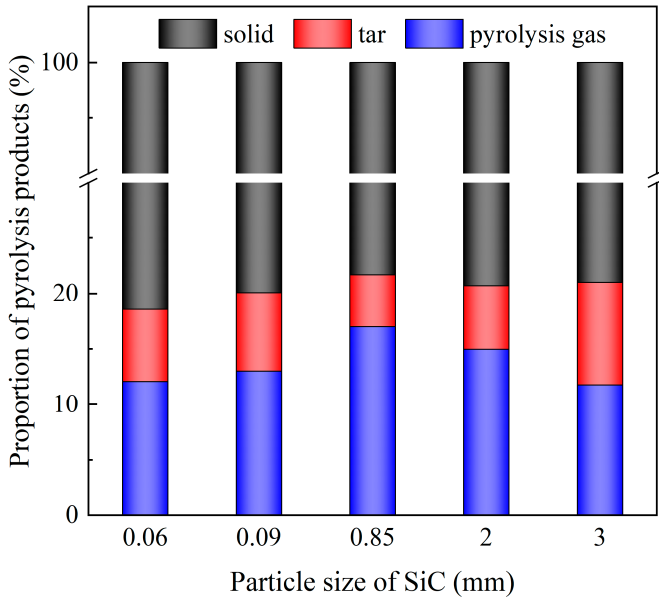

Figure 7. Mass proportion of pyrolysis products at different SiC particle sizes (the SiC loading is 80 g, and microwave power is 600 W).

Concurrently, a comparison of the product mass distribution with particle sizes of 0.06 mm and 0.09 mm and 2 mm and 3 mm revealed that a smaller particle size was conducive to a reduction in tar production and an increase in pyrolysis gas production. In practical industrial applications, it is essential to consider the size of DWTBs and the desired target products in order to achieve the optimal pyrolysis effect, and the relevant characteristics need to be studied further.

3.2.2. Gas Component at Different SiC Size

Figure 8 illustrates the changes in the composition of pyrolysis gas under different SiC particle sizes. When the SiC particle size was small, the primary components of pyrolysis gas were C_2H_4, H_2, etc. As the particle size increased, the content of O_2 decreased, while the content of CO and CH_4 increased. It was speculated that the oxidation reaction of C_2H_4 and H_2 resulted in the production of CO, and that the large-size SiC was conducive to the formation of CH_4 gas. The increase in SiC size was conducive to the occurrence of demethylation reaction and polycondensation reactions, which led to an increase in

CH_4 content. Figure 9 presents the calorific value of pyrolysis gas under different SiC particle sizes and shows heat conversion in relation mass. An intermediate particle size was observed to result in the highest calorific value and heat of pyrolysis gas. SiC with a small particle size exhibited slightly weak wave absorption performance, leading to a low pyrolysis temperature and degree of pyrolysis. Conversely, excessive particle size, although offering good heating performance, had an inadequate specific surface, area leading to a weak heat exchange ability with DWTBs. In the context of actual industrial pyrolysis equipment, it is recommended that SiC of moderate particle size be added in conjunction with the DWTBs to achieve higher energy utilization and a more optimal pyrolysis effect. Furthermore, this approach is conducive to the separation of residual solids and SiC after pyrolysis.

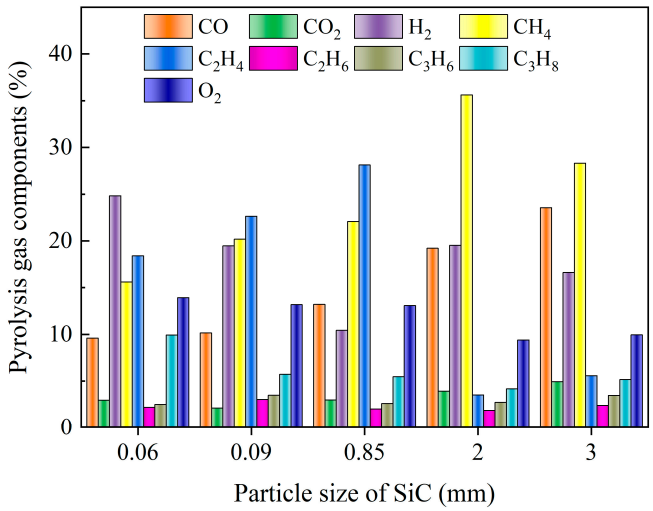

Figure 8. Pyrolysis gas components with different SiC particle sizes (the SiC loading is 80 g, and microwave power is 600 W).

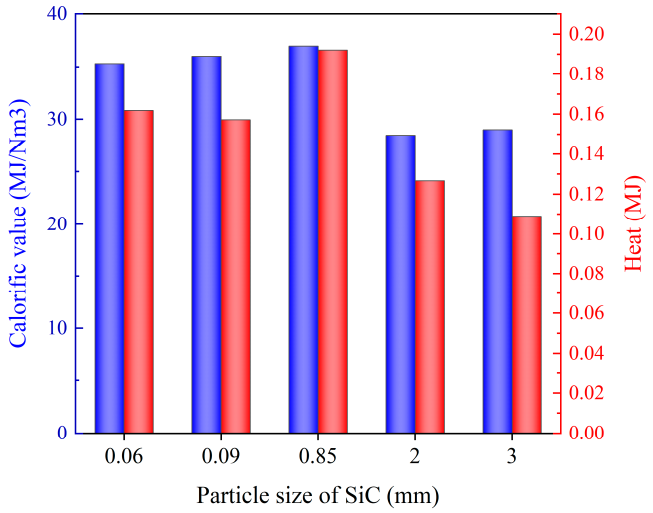

Figure 9. Calorific value and heat of pyrolysis gas with different SiC particle sizes (the SiC loading is 80 g, and microwave power is 600 W).

3.2.3. Temperature Rise Characteristic at Different SiC Size

Figure 10 illustrates the temperature rise curves of material with varying SiC particle sizes. Both the temperature rise rate and the final temperature of the material exhibited an upward trend with the increase in SiC particle size. The final temperatures of the material with the four particle sizes were 539.5 °C, 601.6 °C, 686.4 °C, 731.6 °C and 797.0 °C,

respectively. The initial temperature rise curves of the three groups, which had SiC particle sizes of 0.85 mm, 2 mm, and 3 mm, were basically the same, with the only difference being observed at the final temperature. Similarly, transient temperature drops were observed in several groups of experiments, and the same pattern was observed by Cui et al. [46] during the microwave heating of polypropylene and SiC mixtures. When the SiC particle size was 0.06 mm, the particles were mainly distributed at the bottom of the reactor. As such, the overall heat absorption capacity was poor, the temperature rise was relatively slow, and the temperature distribution inside and outside the blade was relatively uniform, and so the heating and heat dissipation in the later stage of the reaction reached a balance. When the particle size was 0.09 mm, the heating effect was improved, and the distribution of particles and blades was relatively uniform, which was conducive to the secondary pyrolysis of pyrolysis products. Additionally, the heat absorption led to a short decline in temperature, and eventually tended towards being flat. When the particle size continued to increase, the lower specific surface area of a 0.85 mm particle size was not conducive to the occurrence of secondary cracking reactions, meaning there was no obvious temperature drop. The influence of SiC particle size on temperature rise characteristics was the comprehensive result of its wave absorption capacity, pyrolysis reactions, and heat transfer interactions with DWTBs. Studies by Liu et al. [35] proposed that SiC with a medium particle size was conducive to enhancing the conversion rate of polyethylene terephthalate (PET) in the microwave pyrolysis of SiC and PET.

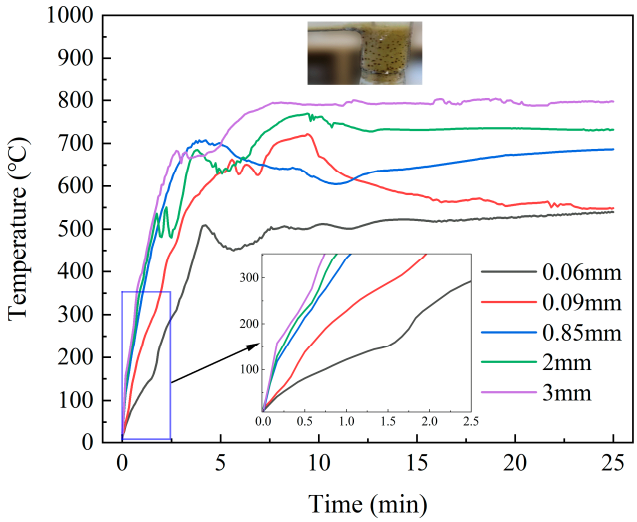

Figure 10. Temperature rise curves of the material with different SiC particle sizes (the SiC loading is 80 g, and microwave power is 600 W).

3.3. Effect of Absorbent (SiC) Loading on Pyrolysis Products

3.3.1. Gas Yield and Oil Yield at Different SiC Loading

Figure 11 illustrates the mass distribution of pyrolysis products under different SiC loadings (for Run 9~Run 13, the SiC particle size is 0.85 mm and microwave power is 600 W). We observed that the absence of SiC resulted in almost no pyrolysis gas and tar production. With the increase in SiC loading, the degree of pyrolysis rose, leading to greater production of pyrolysis gas. The increase in SiC loading enhanced the heat absorption effect of DWTBs. The lowest tar yield (4.7%) was observed at 80 g of SiC loading, while the highest pyrolysis gas yield (17.0%) was recorded. In the experiment, the addition of 80 g SiC basically submerged DWTBs to obtain the best heating effects, with further addition resulting in energy waste. Given that SiC can be recycled in actual use, the amount of SiC added can be controlled in industrial equipment according to the desired target products. In order to achieve a higher degree of pyrolysis and increased pyrolysis gas production, it is crucial to make SiC contact with DWTBs as much as possible. Conversely, if more tar is desired, the amount of SiC needs to be controlled.

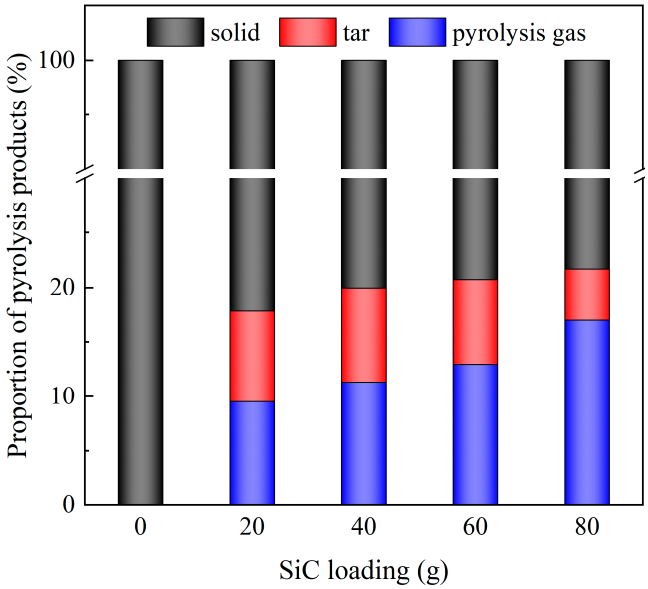

Figure 11. Mass proportion of pyrolysis products under different SiC loadings (the SiC particle size is 0.85 mm, and microwave power is 600 W).

3.3.2. Gas Component at Different SiC Loading

Figure 12 illustrates the distribution of pyrolysis gas components under different SiC loadings. In instances where SiC was not added, the DWTBs exhibited inadequate wave absorption ability and were unable to reach the pyrolysis temperature, resulting in minimal thermal cracking of resin components. Only alterations in the SiC loading had a negligible impact on the composition of the pyrolysis gas. The primary pyrolysis gas in the four groups of experiments was C_2H_4, CH_4, and CO. The production of C_2H_4 was greater when the SiC loading was 80 g. Figure 13 presents the calorific value and the heat converted according to the mass of pyrolysis gas used in each working condition. There was little difference in the calorific value of pyrolysis gas obtained by the four experimental groups. The calorific value of the pyrolysis gas obtained when the SiC loading was 80 g was the largest (36.95 MJ/m^3). The heat of pyrolysis gas was also the highest (0.192 MJ), which was due to the greater quantity of pyrolysis gas produced under this working condition. This could be attributed to the enhanced wave absorption property and heat exchange effect brought by a sufficient amount of SiC. At the same time, the endothermic reaction was enhanced [47] (Resin $\rightarrow$ Char + Tar + Syngas, C + CO_2 $\rightarrow$ 2CO), in accordance with the findings of Fu et al. [48].

3.3.3. Temperature Rise Characteristic at Different SiC Loading

Figure 14 illustrates the temperature rise curves of material with different SiC loadings. In the absence of SiC, only the DWTBs exhibited a slower temperature rise rate, and the final temperature was 418.8 °C, which was insufficient for pyrolysis to occur. The solid obtained after heating is shown as the brown part in Figure 14. The material weight remained essentially unchanged, whereas the solid obtained under other conditions was black. With the increase in SiC loading, both the heating rate and the final temperature in the initial heating stage increased, indicating that more microwave energy was transferred to DWTBs due to SiC addition, resulting in a better cracking effect. In this experiment, when the mass ratio of SiC to DWTBs was 4:1, the heating rate was high, and the pyrolysis degree (mass of pyrolysis gas and tar/mass of original sample) and the calorific value of pyrolysis gas were at their highest levels. The final temperature reached 686.4 °C. The rurther addition of SiC would result in energy waste, and might damage the strength of the glass fiber, thereby reducing its value for subsequent reuse.

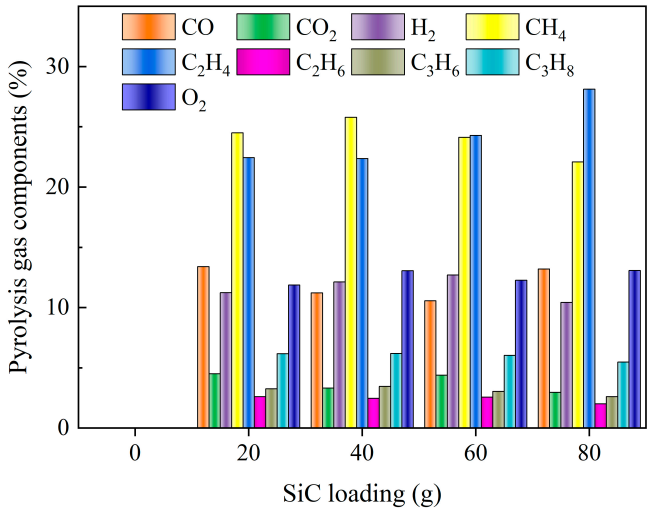

Figure 12. Pyrolysis gas components under different SiC loadings (the SiC particle size is 0.85 mm, and microwave power is 600 W).

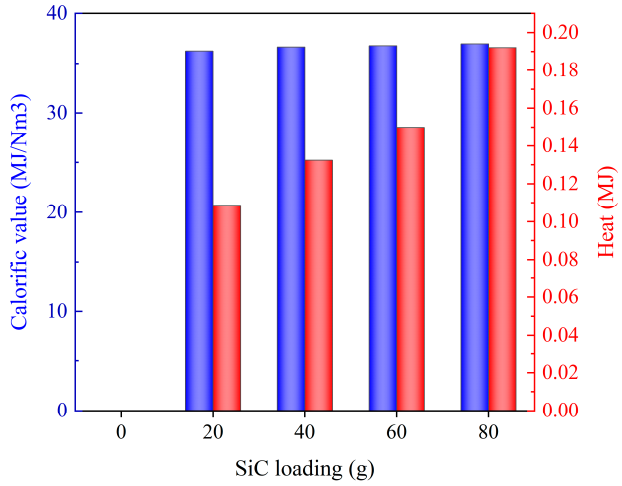

Figure 13. Calorific value and heat of pyrolysis gas under different SiC loadings (the SiC particle size is 0.85 mm, and microwave power is 600 W).

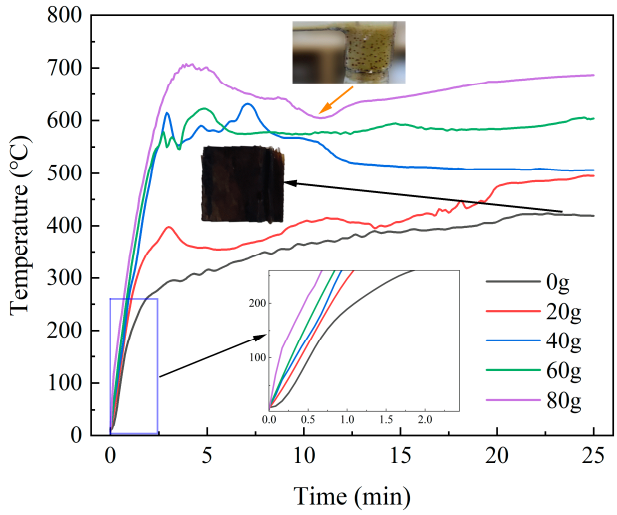

Figure 14. Temperature rise curves of the materials with different SiC loadings (the SiC particle size is 0.85 mm, and microwave power is 600 W).

3.4. Composition Analysis of Pyrolytic Tar

Two groups of typical working conditions were subjected to GC-MS tests, the results of which are depicted in Figure 15. It can be observed that the composition of pyrolysis tar under two conditions was similar, with only slight differences seen in content. The composition of tar was similar to that obtained by Ren et al. [25] in the microwave pyrolysis of carbon-fiber-reinforced composites, except for some large-molecular-weight components, which might be related to the higher microwave pyrolysis temperature seen in this study. In the experiment on Run 5 conditions, the tar yield was the lowest and the pyrolysis degree was the highest. Consequently, there were fewer substances in the tar, and the average molecular weight was relatively low. The tar was predominantly composed of toluene and phenol. However, under Run 7 conditions, the pyrolysis degree was comparatively low, the pyrolysis was insufficient, the composition of tar was more complex, and it contained more high-molecular-weight substances, such as 2-(2-(4-hydroxyphenyl)propan-2-yl)phenol ($C_{15}H_{16}O_2$) and dodecan-1-ol ($C_{12}H_{26}O$), indicating that the macromolecules in the resin were not completely broken down.

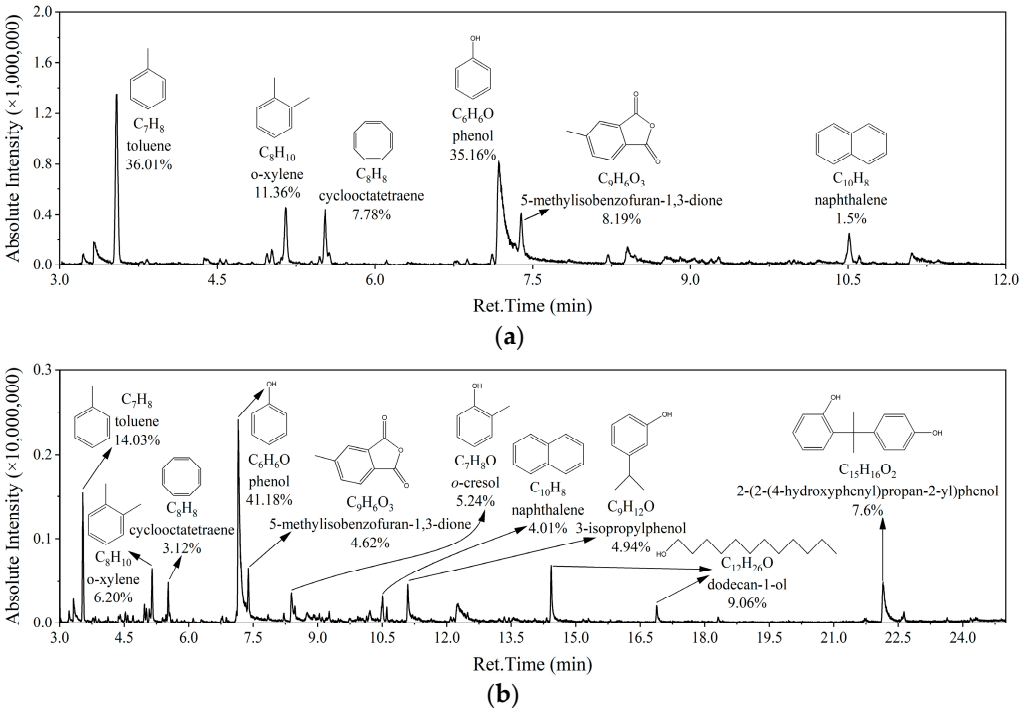

Figure 15. Composition of tar under different experimental conditions: (**a**) Run 5; (**b**) Run 7.

4. Conclusions

This paper presents a study of the microwave pyrolysis characteristics of decommissioned wind turbine blades (DWTBs) with SiC as an absorbent. The glass-fiber-reinforced composite, a typical position in DWTBs, had a glass fiber content of 76.5% and a low calorific value of 7119.7 kJ/kg. The pyrolysis gas components were C_2H_4, CH_4, CO, etc., and phenol and toluene were the main components found in the tar. The results demonstrated that increasing the microwave heating power was conducive to an increase in the heating rate and final temperature, as well as a higher degree of pyrolysis of the material. An increase in microwave heating power from 400 W to 600 W was accompanied by a corresponding increase in the pyrolysis degree, which rose from 15.60% to 21.70%. Concurrently, the heat of pyrolysis gas increased from 0.1115 MJ to 0.19202 MJ. An increase in the particle size of SiC was conducive to improving the heat absorption of the material, while an excessively large particle size caused a poor heat transfer effect. The results of the experiment indicated that the pyrolysis effect was optimal when the particle size of SiC was 0.85 mm, the pyrolysis degree was 21.70%, and the calorific value of pyrolysis gas was the

highest level, which was 36.95351 MJ/m^3. It was observed that almost no pyrolysis of the DWTBs occurred in the case of unloaded SiC. However, with the increase in SiC loading, the pyrolysis degree and heating effect were improved. The pyrolysis gas yield was the highest (17.0%) and tar yield was the lowest (4.7%) when the mass ratio of SiC to DWTBs was 4. Therefore, the optimal process for microwave pyrolysis of decommissioned wind power blades was proposed: microwave heating power of 600 W, SiC particle size of 0.85 mm, and mass ratio of wind turbine blades to SiC of 1:4. These conditions provided data support and a technical reference for the microwave pyrolysis industrial wind turbine blades.

The superiority of pyrolysis lies in the fact that all the products obtained from it have reuse value. After decarbonization, pyrolysis solid can be used for non-woven mats or reinforcing materials such as clutch pedals and roof supports. Tar from pyrolysis has high calorific value and can be used as a candidate fuel for boilers, melting furnaces, and diesel engines. Pyrolysis gas can be used directly for heat production and power generation such as burner ignition or combustion in engines. In conclusion, the microwave pyrolysis of DWTBs can help the wind power industry to achieve sustainable and circular development.

Author Contributions: Writing—original draft, D.Z.; visualization, Q.S.; resources, B.H. and D.T.; Writing—review & editing, M.Z., R.B. and H.Y.; methodology, Y.Z. All authors have read and agreed to the published version of the manuscript.

Funding: This research was funded by the Beijing Natural Science Foundation "Research on circulating fluidized bed combustion reconstruction method and resource utilization of high-aluminum coal ash" (JQ23010).

Data Availability Statement: Data are contained within the article.

Conflicts of Interest: Authors Bo Hou and Da Teng were employed by the company China Energy Longyuan Environmental Protection Co., Ltd. The remaining authors declare that the research was conducted in the absence of any commercial or financial relationships that could be construed as a potential conflict of interest. The China Energy Longyuan Environmental Protection Co., Ltd. had no role in the design of the study; in the collection, analyses, or interpretation of data; in the writing of the manuscript, or in the decision to publish the results.

References

1. GWEC. *Global Wind Report 2022*; GWEC: Brussels, Belgium, 2022.
2. Rodrigues, S.; Restrepo, C.; Kontos, E.; Pinto, R.T.; Bauer, P. Trends of offshore wind projects. *Renew. Sustain. Energy Rev.* **2015**, *49*, 1114–1135. [CrossRef]
3. Staffell, I.; Green, R. How does wind farm performance decline with age? *Renew. Energy* **2014**, *66*, 775–786. [CrossRef]
4. Sieros, G.; Chaviaropoulos, P.; Sørensen, J.D.; Bulder, B.H.; Jamieson, P. Upscaling wind turbines: Theoretical and practical aspects and their impact on the cost of energy. *Wind. Energy* **2012**, *15*, 3–17. [CrossRef]
5. Liu, P.; Barlow, C.Y. Wind turbine blade waste in 2050. *Waste Manag.* **2017**, *62*, 229–240. [CrossRef] [PubMed]
6. Collier, C.; Ashwill, T. Materials and Design Methods Look for the 100-m Blade. *Wind. Eng.* **2011**, *5*, 88–91.
7. Liu, P.; Barlow, C. The environmental impact of Wind Turbine Blades (Presentation). In Proceedings of the 37th Risoe International Symposium on Material Science, Riso, Denmark, 5–8 September 2016.
8. Yang, W.; Kim, K.-H.; Lee, J. Upcycling of decommissioned wind turbine blades through pyrolysis: A review. *J. Clean. Prod.* **2022**, *376*, 134292. [CrossRef]
9. Shen, Y.; Apraku, S.E.; Zhu, Y. Recycling and Recovery of Fiber-Reinforced Polymer Composites for End-of-Life Wind Turbine Blade Management. *Green Chem.* **2023**, *25*, 9644–9658. [CrossRef]
10. Mattsson, C.; André, A.; Juntikka, M.; Tränkle, T.; Sott, R. Chemical recycling of End-of-Life wind turbine blades by solvolysis/HTL. *IOP Conf. Ser. Mater. Sci. Eng.* **2020**, *942*, 012013. [CrossRef]
11. Ge, L.; Xu, C.; Feng, H.; Jiang, H.; Li, X.; Lu, Y.; Sun, Z.; Wang, Y.; Xu, C. Study on isothermal pyrolysis and product characteristics of basic components of waste wind turbine blades. *J. Anal. Appl. Pyrolysis* **2023**, *171*, 105964. [CrossRef]
12. Chen, W.; Ye, M.; Li, M.; Xi, B.; Hou, J.; Qi, X.; Zhang, J.; Wei, Y.; Meng, F. Characteristics, kinetics and product distribution on pyrolysis process for waste wind turbine blades. *J. Anal. Appl. Pyrolysis* **2023**, *169*, 105859. [CrossRef]
13. Kalkanis, K.; Psomopoulos, C.; Kaminaris, S.; Ioannidis, G.; Pachos, P. Wind turbine blade composite materials—End of life treatment methods. *Energy Procedia* **2019**, *157*, 1136–1143. [CrossRef]
14. Ge, L.; Li, X.; Feng, H.; Xu, C.; Lu, Y.; Chen, B.; Li, D.; Xu, C. Analysis of the pyrolysis process, kinetics and products of the base components of waste wind turbine blades (epoxy resin and carbon fiber). *J. Anal. Appl. Pyrolysis* **2023**, *170*, 105919. [CrossRef]

15. Smoleń, J.; Olesik, P.; Jała, J.; Adamcio, A.; Kurtyka, K.; Godzierz, M.; Kozera, R.; Kozioł, M.; Boczkowska, A. The Use of Carbon Fibers Recovered by Pyrolysis from End-of-Life Wind Turbine Blades in Epoxy-Based Composite Panels. *Polymers* **2022**, *14*, 2925. [CrossRef]
16. Wu, Y.; Ge, Z.; Huang, C.; Zha, Z.; Zeng, M.; Ma, Y.; Sun, L.; Hou, Z.; Chu, S.; Zhang, H. In-situ pyrolysis kinetic analysis and fixed-bed pyrolysis behavior of ex-service wind turbine blades. *Waste Manag.* **2023**, *168*, 54–62. [CrossRef]
17. Yousef, S.; Eimontas, J.; Zakarauskas, K.; Striūgas, N. Recovery of styrene-rich oil and glass fibres from fibres-reinforced unsaturated polyester resin end-of-life wind turbine blades using pyrolysis technology. *J. Anal. Appl. Pyrolysis* **2023**, *173*, 106100. [CrossRef]
18. Paulsen, E.B.; Enevoldsen, P. A Multidisciplinary Review of Recycling Methods for End-of-Life Wind Turbine Blades. *Energies* **2021**, *14*, 4247. [CrossRef]
19. Liu, P.; Meng, F.; Barlow, C.Y. Wind turbine blade end-of-life options: An eco-audit comparison. *J. Clean. Prod.* **2018**, *212*, 1268–1281. [CrossRef]
20. Suzuki, T.; Takahashi, J. Prediction of energy intensity of carbon fiber reinforced plastics for mass-produced passenger cars. In Proceedings of the 9th Japan International SAMPE Symposium, Tokyo, Japan, 29 November–2 December 2005; Department of Environmental and Ocean Engineering, The University of Tokyo: Tokyo, Japan, 2005.
21. Deng, J.; Xu, L.; Zhang, L.; Peng, J.; Guo, S.; Liu, J.; Koppala, S. Recycling of carbon fibers from CFRP waste by microwave thermolysis. *Processes* **2019**, *7*, 207. [CrossRef]
22. Åkesson, D.; Foltynowicz, Z.; Christéen, J.; Skrifvars, M. Products obtained from decomposition of glass fibre-reinforced composites using microwave pyrolysis. *Polimery* **2013**, *58*, 582–586. [CrossRef]
23. Åkesson, D.; Foltynowicz, Z.; Christéen, J.; Skrifvars, M. Microwave pyrolysis as a method of recycling glass fibre from used blades of wind turbines. *J. Reinf. Plast. Compos.* **2012**, *31*, 1136–1142. [CrossRef]
24. Hao, S.; He, L.; Liu, J.; Liu, Y.; Rudd, C.; Liu, X. Recovery of carbon fibre from waste prepreg via microwave pyrolysis. *Polymers* **2021**, *13*, 1231. [CrossRef] [PubMed]
25. Ren, Y.; Xu, L.; Shang, X.; Shen, Z.; Fu, R.; Li, W.; Guo, L. Evaluation of mechanical properties and pyrolysis products of carbon fibers recycled by microwave pyrolysis. *ACS Omega* **2022**, *7*, 13529–13537. [CrossRef] [PubMed]
26. Åkesson, D.; Krishnamoorthi, R.; Foltynowicz, Z.; Christ, J.; Kalantar, A.; Skrifvars, M. Glass fibres recovered by microwave pyrolysis as a reinforcement for polypropylene. *Polym. Polym. Compos.* **2013**, *21*, 333–340. [CrossRef]
27. Qiu, T.; Liu, C.; Cui, L.; Liu, H.; Muhammad, K.; Zhang, Y. Comparison of corn straw biochars from electrical pyrolysis and microwave pyrolysis. *Energy Sources Part A Recover. Util. Environ. Eff.* **2023**, *45*, 636–649. [CrossRef]
28. Kremsner, J.M.; Kappe, C.O. Silicon carbide passive heating elements in microwave-assisted organic synthesis. *J. Org. Chem.* **2006**, *71*, 4651–4658. [CrossRef]
29. Ding, D.; Zhou, W.; Zhang, B.; Luo, F.; Zhu, D. Complex permittivity and microwave absorbing properties of SiC fiber woven fabrics. *J. Mater. Sci.* **2010**, *46*, 2709–2714. [CrossRef]
30. Yousef, S.; Eimontas, J.; Striūgas, N.; Abdelnaby, M.A. Influence of carbon black filler on pyrolysis kinetic behaviour and TG-FTIR-GC–MS analysis of glass fibre reinforced polymer composites. *Energy* **2021**, *233*, 121167. [CrossRef]
31. Torres, A.; de Marco, I.; Caballero, B.; Laresgoiti, M.; Legarreta, J.; Cabrero, M.; González, A.; Chomón, M.; Gondra, K. Recycling by pyrolysis of thermoset composites: Characteristics of the liquid and gaseous fuels obtained. *Fuel* **2000**, *79*, 897–902. [CrossRef]
32. Giorgini, L.; Leonardi, C.; Mazzocchetti, L.; Zattini, G.; Cavazzoni, M.; Montanari, I.; Tosi, C.; Benelli, T. Pyrolysis of fiber-glass/polyester composites: Recovery and characterization of obtained products. *FME Trans.* **2016**, *44*, 405–414. [CrossRef]
33. Jing, X.; Dong, J.; Huang, H.; Deng, Y.; Wen, H.; Xu, Z.; Ceylan, S. Interaction between feedstocks, absorbers and catalysts in the microwave pyrolysis process of waste plastics. *J. Clean. Prod.* **2021**, *291*, 125857. [CrossRef]
34. Fan, S.; Zhang, Y.; Cui, L.; Maqsood, T.; Nižetić, S. Cleaner production of aviation oil from microwave-assisted pyrolysis of plastic wastes. *J. Clean. Prod.* **2023**, *390*, 136102. [CrossRef]
35. Liu, Y.; Cui, L.; Liu, H.; Zhao, W.; Zhang, Y. Conversion of polyethylene terephthalate (PET) plastic particles in a microwave-assisted heating reactor. *Int. J. Chem. React. Eng.* **2023**, *21*, 1423–1432. [CrossRef]
36. Fan, S.; Cui, L.; Guang, M.; Liu, H.; Qiu, T.; Zhang, Y. Value-added biochar production from microwave pyrolysis of peanut shell. *Int. J. Chem. React. Eng.* **2023**, *21*, 1035–1046. [CrossRef]
37. Yun, Y.M.; Seo, M.W.; Koo, G.H.; Ra, H.W.; Yoon, S.J.; Kim, Y.K.; Lee, J.G.; Kim, J.H. Pyrolysis characteristics of GFRP (Glass Fiber Reinforced Plastic) under non-isothermal conditions. *Fuel* **2014**, *137*, 321–327. [CrossRef]
38. Grekov, D.; Pré, P.; Alappat, B.J. Microwave mode of heating in the preparation of porous carbon materials for adsorption and energy storage applications—An overview. *Renew. Sustain. Energy Rev.* **2020**, *124*, 109743. [CrossRef]
39. Chen, Y.-R. Microwave pyrolysis of oily sludge with activated carbon. *Environ. Technol.* **2016**, *37*, 3139–3145. [CrossRef] [PubMed]
40. Fagbemi, L.; Khezami, L.; Capart, R. Pyrolysis products from different biomasses: Application to the thermal cracking of tar. *Appl. Energy* **2001**, *69*, 293–306. [CrossRef]
41. Scott, D.S.; Piskorz, J.; Radlein, D. Liquid products from the continuous flash pyrolysis of biomass. *Ind. Eng. Chem. Process Des. Dev.* **1985**, *24*, 581–588. [CrossRef]
42. Feih, S.; Boiocchi, E.; Mathys, G.; Mathys, Z.; Gibson, A.; Mouritz, A. Mechanical properties of thermally-treated and recycled glass fibres. *Compos. Part B Eng.* **2011**, *42*, 350–358. [CrossRef]

43. Ginder, R.S.; Ozcan, S. Recycling of commercial E-glass reinforced thermoset composites via two temperature step pyrolysis to improve recovered fiber tensile strength and failure strain. *Recycling* **2019**, *4*, 24. [CrossRef]
44. Yun, Y.M.; Seo, M.W.; Ra, H.W.; Koo, G.H.; Oh, J.S.; Yoon, S.J.; Kim, Y.K.; Lee, J.G.; Kim, J.H. Pyrolysis characteristics of glass fiber-reinforced plastic (GFRP) under isothermal conditions. *J. Anal. Appl. Pyrolysis* **2015**, *114*, 40–46. [CrossRef]
45. Wu, Z.; Li, C.; Shan, R.; Zhang, J. Synergistic Effects for Co-pyrolysis of Epoxy Resin and Polyurethane from Retired Wind Turbine Blades. *Waste Biomass-Valorization* **2023**, *15*, 1603–1614. [CrossRef]
46. Cui, Y.; Zhang, Y.; Cui, L.; Zhao, W.; Faizan, A. Microwave heating of silicon carbide and polypropylene particles in a fluidized bed reactor. *Appl. Therm. Eng.* **2023**, *232*, 121009. [CrossRef]
47. Zha, Z.; Wang, K.; Ge, Z.; Zhou, J.; Zhang, H. Morphological and heat transfer characteristics of biomass briquette during steam gasification process. *Bioresour. Technol.* **2022**, *356*, 127334. [CrossRef]
48. Fu, W.; Zhang, Y.; Cui, L.; Liu, H.; Maqsood, T. Experimental microwave-assisted air gasification of biomass in fluidized bed reactor. *Bioresour. Technol.* **2023**, *369*, 128378. [CrossRef]